

Seasonal and intraseasonal polar motion variability as deduced from atmospheric torques

Michael Schindelegger^{1,*}, Johannes Böhm¹, David Salstein²

¹Department of Geodesy and Geoinformation, Vienna University of Technology, Gusshausstraße 27–29, 1040 Vienna, Austria

²Atmospheric and Environmental Research Inc, Lexington, MA, U.S.A.

Abstract

Accepted: 23 November 2012
Received: 31 October 2012
Pub. Online: 12 March 2013

Volume: 1
Issue: 2
Page: 89 - 95
November 2012

The main objective of this paper is to investigate the atmospheric excitation of seasonal and intraseasonal polar motion based on the so-called torque approach. For the period 2009–2011, we calculate the comprehensive set of equatorial torques acting on the solid Earth, which arise from pressure gradients at topographic features, frictional wind stresses, and mass-induced forces on the Earth's equatorial bulge. The particular innovation of the study is to use the most recent and accurate meteorological reanalysis data of the ECMWF (European Centre for Medium-Range Weather Forecasts) and the NASA Global Modeling and Assimilation Office for reassessing the ability of atmospheric torques to explain geophysical signals in observed polar motion. Time domain and statistical comparisons suggest that the torque results are of the same quality as the corresponding values from the traditionally applied angular momentum approach. It is shown that the y component of polar motion variability is particularly well accounted for by torques that act over land areas, while the x component also strongly depends on oceanic excitation. A remarkable result is the excellent agreement of the two utilized atmospheric models in terms of torques on all time scales.

Keywords

Earth rotation, Seasonal and intraseasonal polar motion, Geophysical excitation, Atmospheric torques.

Özet

Atmosferik torklardan elde edilen mevsimsel ve mevsim-içi kutup gezinmesi değişimleri

Kabul: 23 Kasım 2012
Alındı: 31 Ekim 2012
Web Yayın: 12 Mart 2013

Cilt: 1
Sayı: 2
Sayfa: 89 - 95
Kasım 2012

Bu makalenin temel amacı mevsimsel ve mevsim-içi kutup gezinmesinin atmosferik eksitasyonunu tork yaklaşımı temelinde incelemektir. Bu çalışmada, 2009-2011 süresince, katı Yer'e etkiyen: topoğrafya üzerindeki atmosfer basınç gradyanlarını, rüzgar sürtünme gerilimlerini ve Yer'in ekvatorial bölgesine etkiyen atmosfer kitlesinin oluşturduğu kuvvetleri içeren bir dizi ekvatorial tork seti hesapladık. Bu çalışmanın kendine özgü yeniliği ise güncel ve duyarlılığı yüksek ECMWF (European Center for Medium-Range Weather Forecast) ve NASA Global Modeling and Assimilation Office meteorolojik analiz verileri kullanılarak ölçülen kutup gezinmeleri içerisindeki jeofizik sinyallerin atmosferik torklar ile açıklanabilme kabiliyetini ortaya koymaktır. Zaman uzayı ve istatistiksel karşılaştırmalar tork sonuçlarının geleneksel açısal momentum yaklaşımından elde edilen ilgili değerleri ile aynı kalitede olduğunu göstermektedir. Kutup gezinmesinin y bileşenindeki değişimlerin karalara etkiyen torklar ile iyi açıklanabildiği, x bileşeninin ise ayrıca okyanussal eksitasyona güçlü bir şekilde bağlı olduğu ortaya konulmuştur. Dikkate değer diğer bir sonuç ise faydalanılan iki atmosfer modelinden tüm zaman ölçekleri için elde edilen torkların mükemmel uyumudur.

Anahtar Sözcükler

Yer dönüklüğü, Mevsimsel ve mevsim-içi kutup gezinmesi, Jeofizik eksitasyon, Atmosferik torklar.

*Corresponding Author: Tel: +43 1 58801 12828 Fax: +43 1 58801 12896

E-mail: michael.schindelegger@tuwien.ac.at (Schindelegger M.), johannes.boehm@tuwien.ac.at (Böhm J.), dsalstei@aer.com (Salstein D.)

1. Introduction

The dynamic interaction of the solid Earth with its fluid envelope (atmosphere, ocean and hydrology) provides one of the major sources for the manifold spatio-temporal variations in Earth rotation (Marcus et al. 2010). The observed fluctuations in the motion of our planet are classically divided into three components: variations of the rotation speed, reckoned in changes in length of day (LOD), the motion of the spin axis in a reference frame tied to the Earth is known as polar motion, and changes in the orientation of this spin axis in a space-fixed reference frame are referred to as precession-nutation (Dehant and de Viron 2002). The observational evidence of geophysical effects in all three parameters has been established in numerous previous studies, see e.g. Gross (2007) for a comprehensive overview. In brief, sub-decadal and non-tidal changes in LOD are almost entirely related to atmospheric dynamics, while polar motion variability at periods from a few days to several years is mainly driven by the atmosphere, the ocean (Gross et al. 2003), and hydrology to a lesser extent (Chen and Wilson 2005). Earth's nutational motion relates chiefly to the gravitational interaction with other celestial bodies, but can be affected by quasi-diurnal atmospheric and oceanic excitation at the level of 0.1 mas (milliarcseconds), see Bizouard et al. (1998). The focus of this paper will be on polar motion variations and their atmospheric origin at seasonal and intraseasonal periodicities.

The impact of dynamical processes in the atmosphere or any mobile fluid on the rotation of the solid Earth is traditionally investigated through the basic principle of angular momentum conservation within the Earth system (Munk and MacDonald 1960). In the last several decades, a host of studies have deployed this angular momentum approach in order to explain geodetic observations of changes in LOD and polar motion in terms of their geophysical origin, see e.g. Rosen and Salstein (1983) or Gross et al. (2003). As angular momentum values can be computed directly from the standard output of established general circulation models and as they are also largely robust with respect to small errors in these analysis fields, the method is particularly fancied. However, it only allows “diagnosing” changes in the angular momentum of the solid Earth and is unable to shed light on the physical processes perturbing Earth rotation (de Viron and Dehant 1999). Such insight can be obtained from an alternative formalism called torque approach, which has been outlined in the comprehensive work of Wahr (1982). Within this method, the atmosphere, the ocean, etc. are conceived as external layers to the mechanical system (de Viron et al. 1999), exerting pressure, friction and gravitational torques on the solid Earth and thus inducing the exchange of angular momentum across the system's interfaces (Fujita et al. 2002). As described by Munk and MacDonald (1960), torque and angular momentum approach are fundamentally equivalent since the torque acting on the fluid layer has to balance the time derivative of its angular momentum (White 1949). This balance has been successfully validated numerous times for atmospheric models on time scales down to 5–10 days, both in the equatorial component (de Viron et al.

1999) and the axial direction (e.g. Swinbank 1985), and will not be treated further.

The primary objective of this paper is to directly quantify the atmosphere's effect on polar motion variations by means of the torque approach. This issue has been addressed in detail by Wahr (1983) and Feldstein (2008), but is generally not sufficiently studied since the comprehensive calculation of all torque terms is considered as a complex task, prone to approximations and sensitive to errors in the underlying circulation models. Evaluating surface forces partly relies on meteorological quantities that are only indirectly supported by observations and have to be parameterized instead (de Viron and Dehant 2003). Moreover, the mathematical formalism relating geophysical excitation to geodetic observations is less advanced for the torque approach, while sophisticated schemes exist for the angular momentum method at long and short periods (Gross 2007; Brzezinski 1994).

In the present study, we relate equatorial atmospheric torques to polar motion at periodicities from 4 to about 400 days based on the output of two established atmospheric analysis systems: ERA-Interim of the ECMWF (European Centre for Medium-Range Weather Forecasts) and MERRA (Modern Era-Retrospective Analysis for Research and Applications) within GEOS-5 (Goddard Earth Observing System Model, Version 5). The results of those models are believed to be superior to previously used analysis fields due to major advances that have been made during the last decade in terms of observation and assimilation techniques as well as spectral resolution and physical parameterization issues. Our use of these improved models can mitigate the possible weaknesses of the torque approach. The core task of this study is thus to derive the various torque terms from the ERA-Interim and MERRA systems and assess the currently achievable agreement between polar motion observations and excitation values based on atmospheric torques. On the time scales investigated here, such an attempt has to be considered along with the oceanic response to air pressure variations by means of the inverted barometer (IB) hypothesis. This approximation should increase the agreement between geodetic observations and torque series.

2. Theoretical background

In classical mechanics a torque is defined as the vector product of an exerted force with its lever arm with respect to a reference axis. By recognizing that the atmosphere (a) couples with the underlying solid Earth (s) via pressure, friction and gravitational forces, one can deduce the three components of the total atmospheric torque

$$\hat{L}^{(a) \rightarrow (s)} = \hat{L}^p + \hat{L}^e + \hat{L}^f \quad (1)$$

as shown by de Viron et al. (1999). Herein, $\hat{L}^{(a) \rightarrow (s)} = L_x^{(a) \rightarrow (s)} + i L_y^{(a) \rightarrow (s)}$ is the complex equatorial interaction torque, separated into three portions: a local pressure or mountain torque \hat{L}^p , an ellipsoidal torque \hat{L}^e and a friction torque \hat{L}^f . Those components and their physical meaning have been discussed extensively in Wahr (1982) or de Viron and Dehant (1999), so that we confine ourselves

to specifying the mathematical expression of the equatorial torque terms in complex notation (cf., Egger and Hoinka 2002; Schindelegger et al. 2013)

$$\hat{L}^p = a^2 \iint (a+h) e^{i\lambda} \left(\frac{dp_s}{d\lambda} \cos\theta - i \frac{dp_s}{d\theta} \sin\theta \right) d\theta d\lambda \quad (2)$$

$$\hat{L}^e = -\frac{i\Omega^2 a^4}{g} \iint p_s e^{i\lambda} \cos\theta \sin^2\theta d\theta d\lambda \quad (3)$$

$$\hat{L}^f = a^3 \iint e^{i\lambda} (i f_\theta - f_\lambda \cos\theta) \sin\theta d\theta d\lambda \quad (4)$$

All three components are understood to be acting on the solid Earth as indicated already in Eq. (1). The quantity $p_s = p_s(\theta, \lambda)$ denotes surface pressure, θ and λ are geographic co-latitude and longitude, a represents Earth's mean radius, g is the nominal gravity acceleration and Ω the mean angular velocity of the rotating reference frame. Here the mountain torque is sensitive to horizontal pressure gradients in both co-latitudinal and longitudinal directions at ellipsoidal heights $h \mathbf{i}\theta \lambda$, whereas the friction torque is dependent on the tangential wind stresses $f_\theta(\theta, \lambda)$ and $f_\lambda(\theta, \lambda)$ also in these two directions. Those two local components however are dominated by the ellipsoidal torque, which combines the pressure and gravitational effects on Earth's bulge (de Viron and Dehant 1999).

Interestingly, \hat{L}^e is formally proportional to the so-called pressure term of atmospheric angular momentum (Bell 1994) – a relationship that is of great use when trying to impose the IB response on the various torque components. As outlined by Marcus et al. (2010), the IB approximation neither affects the friction torque (which is independent of pressure variations) nor the mountain torque. However, the ellipsoidal torque has to be adjusted, i.e. computed from the unmodified surface pressure over land areas and an average pressure value over the world ocean. This correction is exactly the same as for the IB pressure term of atmospheric angular momentum (AAM).

Comparison of the total atmospheric torque to polar motion utilizes a dimensionless complex excitation function $\hat{\phi}$, for which the theoretical basis has been given by Wahr (1982). Here, we resort to Eq. (10) of Fujita et al. (2002), which represents a numerical equivalent of Wahr's torque result

$$\hat{\phi} = \frac{i}{\Omega^2 (C_m - A_m)} \left[1.44 \hat{L}^{(a) \rightarrow (s)} - 0.44 \hat{L}^e \right], \quad (5)$$

where A_m and C_m are the mean equatorial and axial moments of inertia of the mantle. The trailing term of Eq. (5) embodies the effect of load-induced deformations of the solid Earth. Disregarding phenomena with diurnal or higher frequencies, the transfer function relating the equatorial excitation term to polar motion variations $\hat{m} = m_1 + i m_2$ of the instantaneous rotation axis reads (see also Wahr 1982)

$$\hat{m} + \frac{i}{\hat{\sigma}_{cw}} \hat{m} = \hat{\phi}. \quad (6)$$

Herein, $\hat{\sigma}_{cw}$ represents the complex-valued, observed frequency of the Chandler Wobble as specified in Schindelegger et al. (2011). Modern Earth rotation services do not provide the location of the instantaneous rotation pole within the body-fixed reference frame (Gross 2007) but instead report the position $\hat{p} = p_1 + i p_2$ of the so-called celestial intermediate pole (CIP), see Mendes Cerveira et al. (2009) for further details. Hence, the reported polar motion parameters of the CIP need to be converted to variations of the instantaneous rotation pole by means of

$$\hat{m} = \hat{p} - \frac{i}{\Omega} \dot{\hat{p}}. \quad (7)$$

In fact, both poles are nearly identical for frequencies outside the diurnal band (Gross 2007) and one might omit the second term on the right-hand side of Eq. (7). However, we maintain the exact formulation including the small time derivative of the complex CIP trajectory.

3. Data used and their preparation

The investigations of this paper are based on the reanalysis fields of two different atmospheric models for a unified time span of three years (January 2009 to December 2011): (1) the ERA-Interim model which is the current ECMWF global atmospheric reanalysis extending from 1989 to near-real time (Dee et al. 2011); the gridded output from 3-hourly forecast runs has been used to obtain surface pressure and instantaneous stress vectors at $0.5^\circ \times 0.5^\circ$ horizontal resolution, and (2) the MERRA model as the major new reanalysis of NASA for the satellite era built on the Goddard Earth Observing System Data Assimilation System Version 5 (GEOS-5), see Rienecker et al. (2011): this model provides 3-hourly surface pressure values at grid points with 1.25° latitudinal and longitudinal intervals as well as hourly flux data on a $0.5^\circ \times 0.6^\circ$ grid. In addition, for both ERA-Interim and MERRA a static surface geopotential field describing the topography were downloaded and converted to ellipsoidal heights at the given resolution.

By applying Eqs. (2) – (4) in their discretized form, the equatorial pressure torques, ellipsoidal torques and friction torques were computed at the time resolution of the underlying meteorological fields. Note that the surface pressure fields required for \hat{L}^p differ from that used in \hat{L}^e due to the IB correction. In order to unify the considerations as well as to focus on seasonal and intraseasonal periodicities, we adopted an appropriate low pass filter (5th order Butterworth) with cut-off frequency at 0.5 cycles per day (cpd) and resampled the resulting time series at daily intervals. This procedure is consistent with the sampling of the so-called C04-solution of the IERS (International Earth Rotation and Reference Systems Service, see Gambis (2012)), which serves as reference for the observed polar motion from 2009 to 2011.

4. Comparison of atmospheric torques and observed polar motion

As a first analysis step, it proves interesting to take a look at the magnitude of all torque constituents at various frequency bands (Figure 1). The two-sided spectra, each obtained

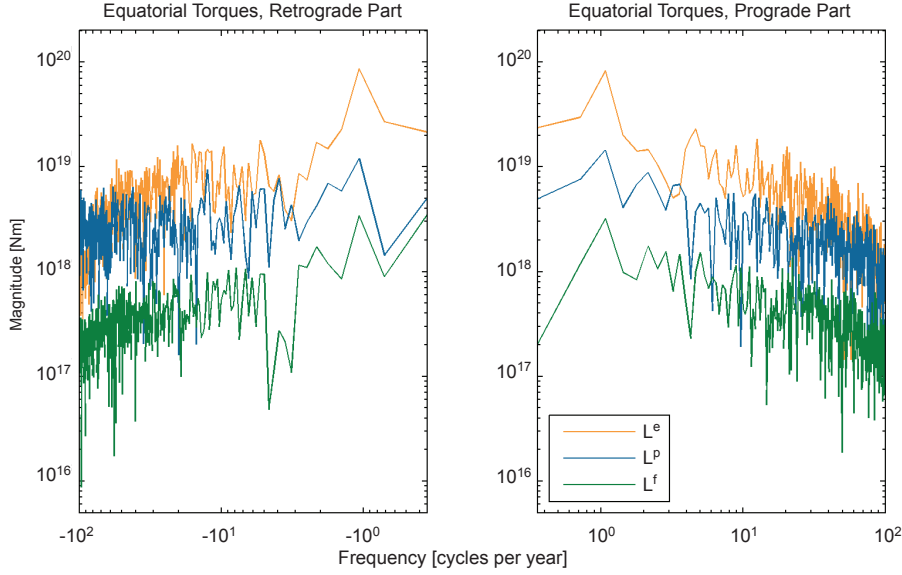


Figure 1: Power spectrum of the equatorial torque terms separated into a retrograde part (left panel) and a prograde part (right panel): ellipsoidal torque (orange line), mountain torque (blue line) and friction torque (green line) as computed from the output of ERA-Interim.

from a 2^{10} -point discrete Fourier transform of the complex torque signals from ERA-Interim, reveal the dominance of the ellipsoidal torque on nearly all time scales, explaining 50–90% of the total torque variance. Distinct pro- and retrograde annual wobbles in \hat{L}^e are readily apparent, albeit their amplitudes have been reduced due to the IB correction. The mountain torque \hat{L}^p holds substantial power throughout, particularly as shorter periodicities are approached, whereas the friction torque \hat{L}^f appears to be almost one order of magnitude smaller than \hat{L}^p . At the lowest frequencies calculated, which include the seasonal bands, the magnitude of all terms is larger than at higher frequencies, including the friction torque term, which then becomes comparable to the mountain torque in the retrograde part of the spectrum.

Comparing observed polar motion to the total interaction torque requires converting the time series of C04-parameters $x_p = p_1$ and $y_p = -p_2$ to the geodetic excitation torque $\hat{\phi} = \hat{\phi}^{(g)}$ based on Eqs. (6) and (7). Herein, the time derivatives of \hat{p} and \hat{m} can be approximated by central differences in both the x and y components. The geophysical (atmospheric) counterpart of $\hat{\phi}^{(g)}$ is labeled $\hat{\phi}^{(a)}$ and was easily determined from Wahr’s torque expression in Eq. (5).

Figures 2 and 3 provide the time domain comparison between observed and modeled excitation values in x and y direction, incorporating results from both ERA-Interim and MERRA. The most clear-cut signal in observational data is an annual term of amplitude 26 mas in $\phi_y^{(g)}$ (Figure 3a), which is the excitation component known to be more sensitive to substantial variations of air pressure over land areas, see de Viron et al. (2002). Given this relationship, it is comprehensible that the atmospheric excitation $\phi_y^{(a)}$ (Figure 3b) accounts for 91% of the observed annual variance in $\phi_y^{(g)}$. The residual signal $\phi_y^{(g)} - \phi_y^{(a)}$ (Figure 3c) is thus dominated by intraseasonal fluctuations, which arise from the fact that atmospheric processes typically explain 40–60% of the vari-

ance in $\phi_y^{(g)}$ at periodicities from 4 to 100 days, cf. Feldstein (2008). Note too that similar values were derived by Gross (2003) based on the angular momentum approach. Further statistical measures, specified in Table 1, include the correlation coefficient ρ between geodetic and atmospheric excitation functions as well as the root mean square (r.m.s.) value of the residuals $\phi_y^{(g)} - \phi_y^{(a)}$. ERA-Interim and MERRA yield virtually identical results: r.m.s. values at the level of 27.3 mas (as opposed to 44.6 mas in the raw observed excitation function $\phi_y^{(g)}$) and $\rho = 0.79$, which is very close to the correlation coefficient inferable from the angular momentum approach ($\rho = 0.80$), see the interactive plotting tools of Gambis (2012) for the same time span 2009–2011.

On the contrary, the polar motion excitation function in the x direction (Figure 2a) is characterized by smaller overall amplitudes and likewise weak seasonal signals; the annual wobble being only of 7 mas in magnitude. The smallness of those effects is linked to the location of the $\phi_x^{(g)}$ weighting patterns, which are mainly centered over oceanic areas with generally weaker annual or semi-annual air pressure variability that is further reduced by the IB effect (Marcus et al. 2010). Considerable intraseasonal variations exist, however, and those can be partly ascribed to atmospheric excitation $\phi_x^{(a)}$ (Figure 2b). Detailed analysis of the spectral content of geodetic and atmospheric time series between 4 and 100 days yielded an averaged explained variance in $\phi_x^{(g)}$ of 55%.

Table 1: Correlation coefficient ρ between observed and modeled excitation functions in x and y direction, as well as root mean square values of the respective differences in mas for both the ERA-Interim model and MERRA.

	ERA-Interim		MERRA	
	ρ	r.m.s [mas]	ρ	r.m.s [mas]
x	0.60	18.6	0.60	18.6
y	0.79	27.3	0.79	27.4

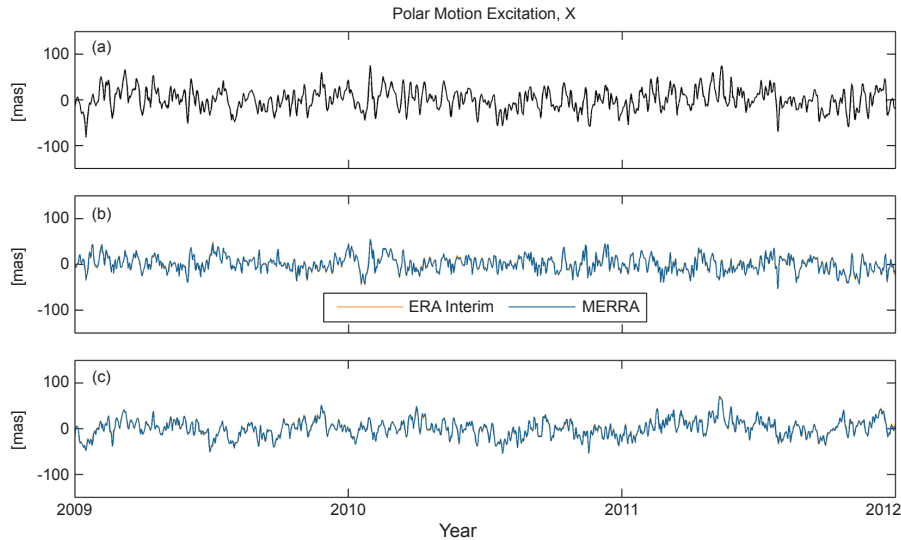


Figure 2: Comparison of (a) observed polar motion excitation in x direction (black line) and (b) modeled excitation from atmospheric torques: ERA-Interim (orange line) and MERRA (blue line). (c) Residuals for both models after subtracting atmospheric excitation from geodetic excitation. A constant offset of +88.0 mas has been removed from the geodetic excitation function.

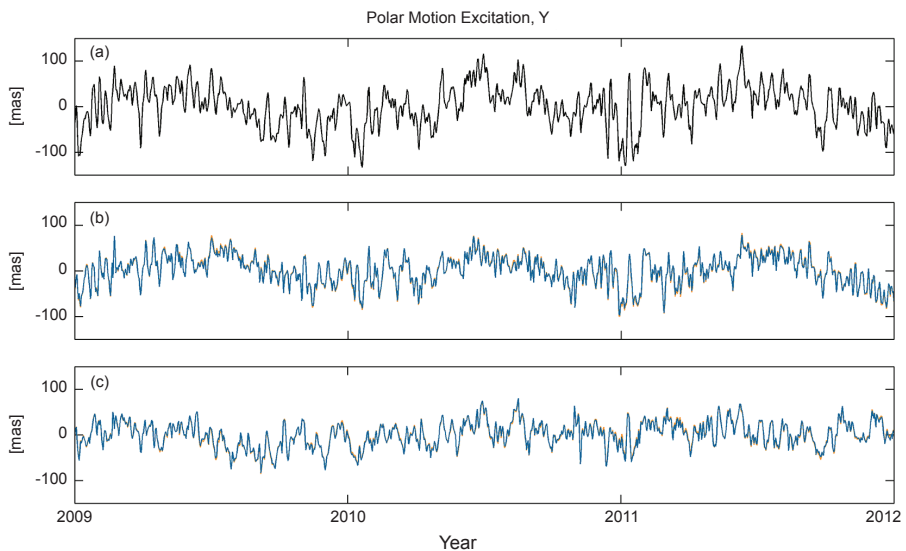


Figure 3: Comparison of (a) observed polar motion excitation in y direction (black line) and (b) modeled excitation from atmospheric torques: ERA-Interim (orange line) and MERRA (blue line). (c) Residuals for both models after subtracting atmospheric excitation from geodetic excitation. A constant offset of -337.4 mas has been removed from the geodetic excitation function.

The remaining portion $\phi_x^{(g)} - \phi_x^{(a)}$ is depicted in Figure 2c and features an r.m.s value of 18.6 mas for both ERA-Interim and MERRA (as opposed to 23.0 mas in the raw observed excitation function $\phi_x^{(g)}$), see Table 1. Consistent with the aforementioned importance of oceanic processes, the correlation coefficient between $\phi_x^{(g)}$ and atmosphere-alone excitation functions is found to be only $\rho = 0.60$. Yet again, these statistical measures obtained from the torque approach are certainly no worse than the corresponding values of the angular momentum approach (Gross 2003; Gambis 2012).

In support of the time series plots and the given numerical values, Figure 4 provides an illustration of the complex polar motion excitation function $\hat{\phi}^{(g)}$ and its residuals after

subtraction of the ERA-Interim torques in the spectral domain. The underlying Fourier transform was performed with the same settings as that shown in Figure 1, but for reasons of clarity the cut-off frequency in Figure 4 corresponds to a period of 10 days. The main statements from the analysis in the time domain are now visible at pro- and retrograde frequencies, most notably the overall reduction of amplitudes in $\hat{\phi}^{(g)}$ by a factor of two (or $2 \cdot 10^0$) as well as the remarkable dip from 17 mas to 6 mas at the prograde annual frequency after subtracting the influence of the atmosphere. Intraseasonal wobbles at retrograde frequencies of 10–20 cycles per year are particularly well accounted for by atmospheric torques and confirm similar findings of Feldstein (2008), who also stressed the dominant role of the ellipsoidal torque at such

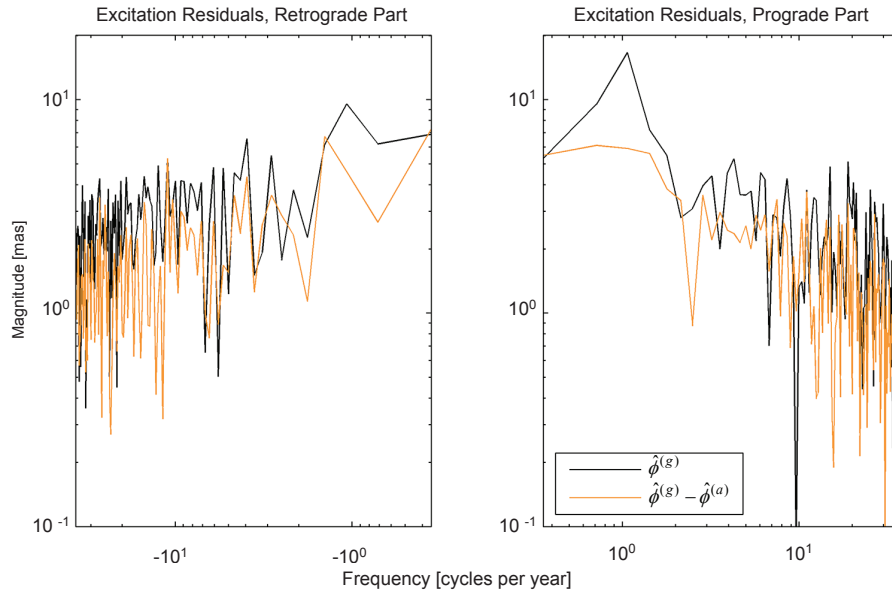


Figure 4: Power spectrum of the equatorial excitation function separated into a retrograde part (left panel) and a prograde part (right panel): observed polar motion excitation $\hat{\phi}^{(g)}$ (black line), and residuals $\hat{\phi}^{(g)} - \hat{\phi}^{(a)}$ (orange line) after subtraction of ERA-Interim torques.

periodicities. Nonetheless, the remaining spectral peaks at the level of 2–6 mas illustrate that explaining observed polar motion variability solely by atmospheric torques and an IB ocean is only a partial solution to the problem of closing Earth’s excitation budget. Within the framework of the angular momentum approach, numerous studies (e.g. [Chen and Wilson 2005](#); [Dobslaw et al. 2010](#)) have shown that a combined geophysical excitation deduced from numerical models of atmosphere, ocean and continental hydrosphere yields a significantly better agreement with geodetic results. Remaining discrepancies in the seasonal and intraseasonal excitation budget are generally attributed to unconsidered dynamical processes as well as uncertainties and inconsistencies in the deployed circulation models ([Dobslaw et al. 2010](#)). Theoretically, similar considerations involving a combination of fluids should be possible for the torque approach. In this respect, our work indicates that torques from ERA-Interim and MERRA provide a realistic measure of the actual atmospheric excitation. However, dynamic ocean models still need major improvements and the backing of bathymetry observations in order to produce reliable torque terms.

Finally, an interesting result from our graphical and statistical comparisons is that the excitation functions produced by ERA-Interim and MERRA are almost identical. Such a great level of coherence between the torque terms (1.00 for \hat{L}_e , 0.98 for \hat{L}_p and 0.90 for \hat{L}_f at intraseasonal frequencies, not depicted) from different atmospheric models exceeds that of previous studies, e.g. [de Viron and Dehant \(2003\)](#), and will be further investigated in a future publication. This close match is probably also larger than the agreement of models in terms of AAM values, which are affected by the uncertainty of vertical wind profiles. The deduced coherence values suggest that ERA-Interim and MERRA perform very similarly with regard to global and local patterns of surface

pressure. In this respect, it should be acknowledged that the surface pressure output of atmospheric models is well-constrained by meteorological observations, which are certainly common to both ERA-Interim and MERRA.

5. Conclusion and outlook

We have recalled the basic formalism for studying the geophysical excitation of polar motion by means of torques exerted by the atmosphere on the solid Earth and an IB ocean. The numerical implementation of this torque approach based on forecast data of ERA-Interim and MERRA yielded a level of agreement between observed and modeled excitation which can be compared to that usually obtained from the angular momentum approach (see the interactive plotting tools provided by [Gambis \(2012\)](#)). A large portion of this similarity in the performance of both methods (angular momentum and torques) is due to the formal equivalence of the pressure term in AAM and the ellipsoidal torque, which explains 50–90% of the total torque variance on time scales down to 10 days. Although atmospheric dynamics is the main driving agent for seasonal and intraseasonal polar motion variability, a non-negligible contribution is due to the ocean, i.e. its pressure- and wind-induced non-tidal variations. Hence, a modeling approach encompassing both atmospheric and oceanic torques should be adopted for a better chance at increasing the match between geodetic and geophysical quantities. At present, such an effort is clearly restricted by the uncertainties of dynamic oceanic models in terms of pressure and friction values at the bathymetry. On the contrary, atmospheric torques from ERA-Interim and MERRA have been found to be impeccably coherent. We consider this finding to be a clear indication for the reliability of torque series from current atmospheric models. A possible extension to the work presented here would be to analyze the underlying forcing fields of the various torque terms in order to assess the ori-

gin and location of the physical processes responsible for the substantial variations in observed polar motion.

Acknowledgements

This work was accomplished within project P20902-N10 of the Austrian Science Fund (FWF). Co-author David Salstein is supported in part by Grant ATM-091370 from the U.S. National Science Foundation (NSF). We greatly acknowledge the use of meteorological data of the ECMWF and the NASA Global Modeling and Assimilation Office. We are also grateful for the valuable recommendations of the two reviewers and likewise appreciate the efforts of K. Teke, who translated this paper into Turkish.

References

- Bell M.J., (1994), *Oscillations in the equatorial components of the atmosphere's angular momentum and torques on the earth's bulge*, Q. J. R. Meteorol. Soc., 120,195–213.
- Bizouard C., Brzeziński A., Petrov S., (1998), *Diurnal atmospheric forcing and temporal variations of the nutation amplitudes*, J. Geod., 72,561–577.
- Brzeziński A., (1994), *Polar motion excitation by variations of the effective angular momentum function, II: extended-model*, Manuscripta Geodetica, 19,157–171.
- Chen J., Wilson C., (2005), *Hydrological excitation of polar motion, 1993–2002*, Geophys. J. Int., 160,833–839, doi: 10.1111/j.1365-246X.2005.02522.x.
- Dee D.P. et al., (2011), *The ERA-Interim reanalysis: configuration and performance of the data assimilation system*, Q. J. R. Meteorol. Soc., 137,553–597, doi:10.1002/qj.828.
- de Viron O., Dehant V., (1999), *Earth's rotation and high frequency equatorial angular momentum budget of the atmosphere*, Surv. Geophys., 20,441–462.
- de Viron O., Dehant V., (2003), *Tests on the validity of atmospheric torques on Earth computed from atmospheric model outputs*, J. Geophys. Res., 108(B2),2068, doi: 10.1029/2001JB001196.
- de Viron O., Bizouard C., Salstein D., Dehant V., (1999), *Atmospheric torque on the Earth and comparison with atmospheric angular momentum variations*, J. Geophys. Res., 104(B3),4861–4875, doi: 10.1029/1999JB900063.
- de Viron O., Dickey J.O., Marcus, S.L., (2002), *Annual atmospheric torques: Processes and regional contributions*, Geophys. Res. Lett., 29(7),1140, doi: 10.1029/2001GL013859.
- Dehant V., de Viron O., (2002), *Earth rotation as an interdisciplinary topic shared by astronomers, geodesists and geophysicists*, Adv. Space Res., 30(2),163–173.
- Dobslaw H., Dill R., Grötzsch A., Brzeziński A., Thomas M., (2010), *Seasonal polar motion excitation from numerical models of atmosphere, ocean and continental hydrosphere*, J. Geophys. Res., 115(B10406), doi: 10.1029/2009JB007127.
- Egger J., Hoinka K.P., (2002), *Equatorial components of global atmospheric angular momentum: Covariance functions*, Q. J. R. Meteorol. Soc., 128,1137–1157.
- Feldstein S., (2008), *The dynamics of atmospherically driven intraseasonal polar motion*, J. Atm. Sciences, 65(7),2290–2307.
- Fujita M., Chao B.F., Sanchez B.V., Johnson T.J., (2002), *Oceanic torques on solid Earth and their effects on Earth rotation*, J. Geophys. Res., 107(B7),2154, doi: 10.1029/2001JB000339.
- Gambis D., (2012), *Earth Orientation Center, Observatoire de Paris*, <http://hpiers.obspm.fr/eop-pc/>, as at September 2012.
- Gross R.S., Fukumori I., Menemenlis D., (2003), *Atmospheric and oceanic excitation of the Earth's wobbles during 1980–2000*, J. Geophys. Res., 108(B8),2370, doi: 10.1029/2002JB002143.
- Gross R.S., (2007), *Earth rotation variations – long period*, In: *Treatise on Geophysics*, Vol. 3, Geodesy, (Herring T.A., Ed.), Elsevier, pp. 239–294.
- Marcus S.L., de Viron O., Dickey, J.O., (2010), *Interannual atmospheric torque and El-Niño-Southern Oscillation: Where is the polar motion signal?*, J. Geophys. Res., 115(B12409), doi: 10.1029/2010JB007524.
- Mendes Cerveira P., Böhm J., Schuh H., Klügel T., Velikoseltsev A., Schreiber U., Brzeziński A., (2009), *Earth rotation observed by Very Long Baseline Interferometry and ring laser*, Pure Appl. Geophys., 166,1499–1517.
- Munk W.H., MacDonald G.J.F., (1960), *The Rotation of the Earth: A Geophysical Discussion*, Cambridge University Press, New York.
- Rienecker M.M. et al., (2011), *MERRA – NASA's Modern-Era Retrospective Reanalysis for Research and Applications*, J. Climate, 24(17),3624–3648.
- Rosen R.D., Salstein D.A., (1983), *Variations in atmospheric angular momentum on global and regional scales and the length of day*, J. Geophys. Res., 88(C9),5451–5470.
- Schindelegger M., Böhm J., Salstein D., Schuh H., (2011), *High-resolution angular momentum functions related to Earth rotation parameters during CONT08*, J. Geod., 85(7),425–433, doi: 10.1007/s00190–011–0458–y.
- Schindelegger M., Böhm S., Böhm J., Schuh H., (2013), *Atmospheric Effects on Earth Rotation*, In: *Atmospheric Effects in Space Geodesy*, (Böhm J., Schuh H., Eds.), Springer, in press.
- Swinbank R., (1985), *The global atmospheric angular momentum balance inferred from analyses made during FGGE*, Quart. J. R. Met. Soc., 111,977–992.
- Wahr J.M., (1982), *The effects of the atmosphere and the oceans on the Earth's wobble – I. Theory*, Geophys. J. R. Astron. Soc., 70,349–372.
- Wahr J.M., (1983), *The effects of the atmosphere and the oceans on the Earth's wobble and on the seasonal variations in the length of day – II. Results*, J. R. Astron. Soc., 74,451–487.
- White R.M., (1949), *The role of the mountains in the angular-momentum balance of the atmosphere*, J. Atmos. Sci., 6(5), 353–355.